ChemComm

COMMUNICATION

View Article Online
View Journal | View Issue

Cite this: *Chem. Commun.*, 2023, **59**, 5745

Received 13th February 2023,
Accepted 15th April 2023

DOI: 10.1039/d3cc00665d

rsc.li/chemcomm

Attenuation of α-synuclein aggregation by catalytic photo-oxygenation†

Atsushi Iwai,[a] Reito Nakamura,[b] Ikumi Tomizawa,[b] Harunobu Mitsunuma,[a] Yukiko Hori,[b] Taisuke Tomita,[b] Youhei Sohma *[c] and Motomu Kanai *[a]

We developed catalyst 11 to promote selective photo-oxygenation of α-synuclein amyloid and attenuate its aggregation. Catalyst 11 effectively oxygenated both small and large aggregates. The oxygenated α-synuclein exhibited lower seeding activity than intact α-synuclein. This study corroborates the feasibility of catalytic photo-oxygenation as an anti-synucleinopathy strategy.

Synucleinopathies, including Parkinson's disease, dementia with Lewy bodies and multiple system atrophy, are neurodegenerative diseases of the central nervous system. The cause of synucleinopathies involves aggregation of α-synuclein (α-syn) in the brain.[1–3] α-Syn is an intracellular protein consisting of 140 amino acid residues. The α-syn monomer is non-toxic, but its aggregated form, called amyloid, is toxic. α-Syn amyloid[4] includes soluble oligomers and insoluble fibrils composed of small and large aggregates, respectively. While insoluble fibrils of α-syn composed of large aggregates form the Lewy bodies and Lewy neurites, the soluble oligomers are more neurotoxic than the insoluble fibrils.[5,6] α-Syn aggregation spreads throughout the brain by propagation among neurons.[7–9] The propagation is mediated by small fibrils generated from the fibril ends, acting as seeds to facilitate α-syn aggregation within neurons. The seeding activity of small aggregates is critical in the pathogenesis of synucleinopathies. Therefore, the development of therapies that target oligomers and small fibrils of α-syn may be an effective treatment of synucleinopathies.

We previously developed amyloid-selective photo-oxygenation catalysts **1–4**, targeting amyloid-β peptide (Aβ) and tau protein (tau) (Fig. 1a).[10–13] Catalysts **1–4** comprised a switching function to detect the cross-β sheet structure characteristic to amyloids and selectively exerted oxygenation activity by binding with amyloids under photo-irradiation. Photo-oxygenation of Aβ reduced its toxicity and enhanced phagocytotic degradation in living mice brains.[14] Photo-oxygenation of tau by catalyst **3** attenuated the seeding activity that precedes amyloid formation.[12] Despite their amyloid-selectivity, the catalytic activities of **1–4** were turned on by binding with large aggregates, not by small aggregates. Moreover, catalyst activities toward α-syn have not been systematically studied. Here, we disclose that photo-oxygenation catalyst **11** successfully attenuates the aggregation of α-syn. Catalyst **11**

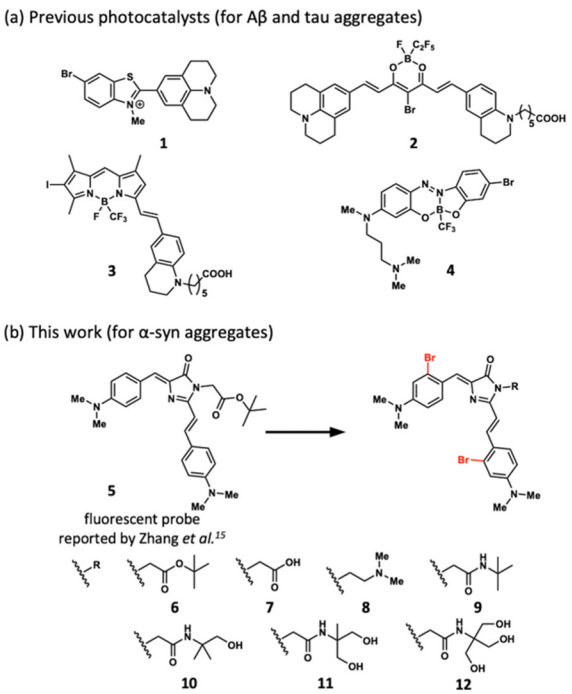

Fig. 1 Structures of photo-oxygenation catalysts (**1–4**, **6–12**) and fluorescent probe **5**.

[a] *Laboratory of Synthetic Organic Chemistry, Graduate School of Pharmaceutical Sciences, The University of Tokyo, 7-3-1 Hongo, Bunkyo-ku, Tokyo 113-0033, Japan. E-mail: kanai@mol.f.u-tokyo.ac.jp*
[b] *Laboratory of Neuropathology and Neuroscience, Graduate School of Pharmaceutical Sciences, The University of Tokyo, 7-3-1 Hongo, Bunkyo-ku, Tokyo 113-0033, Japan*
[c] *School of Pharmaceutical Sciences, Wakayama Medical University, 25-1 Shichiban-cho, Wakayama 640-8156, Japan. E-mail: ysohma@wakayama-med.ac.jp*

† Electronic supplementary information (ESI) available: Experimental details and supplementary figures. See DOI: https://doi.org/10.1039/d3cc00665d

oxygenated small aggregates of α-syn with comparably high efficiency to large aggregates.

Zhang *et al.* previously reported that an amyloid-sensing fluorescence probe **5** (Fig. 1b), designed based on the green fluorescent protein (GFP) chromophore, could detect small aggregates of α-syn.[15,16] We hypothesized that photo-oxygenation catalysts based on **5** would furnish high photo-oxygenation activity for small aggregates of α-syn.

Probe **5** is composed of two electron donors (*N*,*N*-dimethylaniline) and an electron acceptor (imidazolone) moieties, connected to each other by single bonds. In the absence of amyloid, the excited state of **5** generated after photo-irradiation relaxes to the ground state *via* a twisted intramolecular charge transfer state through a non-radiative pathway. In the presence of amyloid, however, the single-bond rotation between the donor and acceptor moieties of **5** is inhibited by binding. Therefore, the photoexcited probe fluoresces when it returns to the ground state. Based on previous reports,[10–12] we hypothesized that introducing bromine atoms to **5** accelerates inter-system crossing due to heavy atom effects and furnishes amyloid-dependent photo-oxygenation activity (Fig. 1b, **6**). To improve water solubility, we synthesized various derivatives by introducing polar functional groups, such as carboxylic acid, amine, and hydroxy groups (Fig. 1b, **7**–**12**). Binding affinities of those catalysts to aggregated α-syn were confirmed by a quartz crystal microbalance method (K_d = 2.6–39 μM: Fig. S1, ESI†).

To aggregated α-syn in PBS (69 μM, pH 7.4), which was generated through pre-incubation at 37 °C for 24 h, a catalyst (20 μM) was added. The mixture was irradiated with green light (λ = 500 nm, Fig. S2 and S3, ESI†) at 37 °C for 30 min. After tryptic digestion, oxygenation yields of three resulting peptide fragments (Fig. 2a, 1–6, 46–58, and 103–140) were determined using LC-MS (Fig. 2b). The new catalysts promoted photo-oxygenation of methionine and histidine residues of α-syn (Fig. 2c). Catalyst **11** containing di-hydroxy *tert*-butyl amide showed the highest photo-oxygenation yield (Fig. 2c). Therefore, further studies were conducted using **11**.

Next, the α-syn amyloid selectivity of **11** was examined (Fig. 2d and e). Riboflavin[17] exerting the oxygenation activity regardless of the presence or absence of amyloid, was used for comparison. First, the photo-oxygenation reaction using **11** or riboflavin was performed with α-syn aggregates and three non-amyloid peptides, angiotensin IV (AT4), leuprorelin (LeuP), and met-enkephalin (ME). Riboflavin promoted oxygenation not only for α-syn aggregates (22% yield) but also for other three non-amyloid peptides (AT4: 19%, LeuP: 22%, ME: 53%), whereas catalyst **11** showed marked oxygenation activity only for α-syn aggregates (51% yield) but not for other peptides (less than 1.8%) (Fig. 2d). Furthermore, the catalytic photo-oxygenation was carried out using a mixture of α-syn aggregates, AT4, LeuP, and ME at equimolar concentrations. While riboflavin oxygenated all the substrates to a similar extent (~20% yield), catalyst **11** produced significantly higher oxygenation yield for α-syn aggregates than other peptides (Fig. 2e). Photo-oxygenation with **11** hardly proceeded to monomer α-syn (Fig. S5, ESI†). These results indicate that catalyst **11** possesses high α-syn amyloid selectivity. The amyloid selectivity is likely due to the photo-induced singlet oxygen ($^1O_2$) production through the inhibition of molecular motion of the catalyst by binding with amyloid (Fig. S6–S8, ESI†), a similar mechanism to our previous photo-oxygenation catalysts **1**–**3**.[10–12] The oxygenation activity of catalyst **11** to aggregated α-syn was higher than that to aggregated amyloid β (Fig. S9, ESI†), suggesting the selectivity between amyloids by **11**.

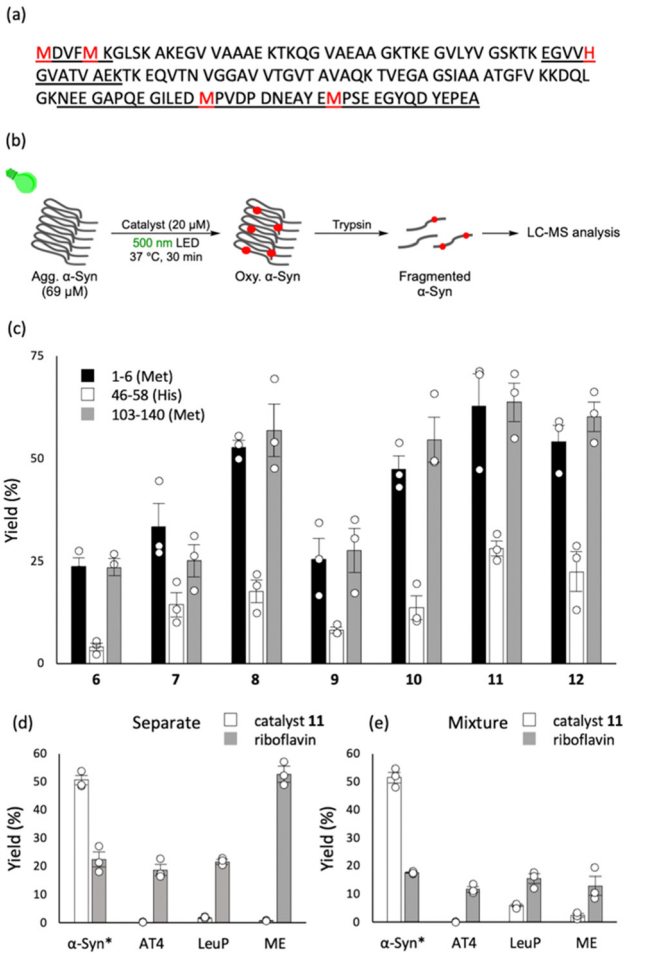

Fig. 2 (a) Amino acid sequence of α-syn. Methionine (M) and histidine (H) residues that potentially undergo oxygenation are highlighted with red colour. Peptide fragments obtained after trypsin digestion are underlined. (b) Reaction conditions for photo-oxygenation of α-syn amyloid. A PBS (pH 7.4) solution containing α-syn (69 μM; aggregated sample was prepared *via* incubation at 37 °C for 24 h) and catalyst (20 μM) was photo-irradiated (λ = 500 nm) at 37 °C for 30 min. The reaction mixture was treated with Trypsin Gold and peptide fragments were analysed using LC-MS. (c) Photo-oxygenation yield of α-syn amyloid (n = 3, mean ± SEM). Almost no oxygenation progressed in the catalyst only sample and in the light only sample (see Fig. S4, ESI†). (d) A PBS solution (pH 7.4) containing aggregated α-syn, angiotensin-IV (AT4; amino acid sequence with underlined potential oxidation sites: VYIHPF), leuprorelin (LeuP; Pyro-EHWSYLLRP), or met-enkephalin (ME; YGGFM) (20 μM each) and catalyst **11** (4 μM) or riboflavin (4 μM) was photo-irradiated (λ = 500 nm) at 37 °C for 30 min, and each reaction mixture was analysed by LC-MS (n = 3, mean ± SEM, *: oxygenation yield at α-syn (1–6)). (e) A PBS solution (pH 7.4) containing a mixture of aggregated α-syn, AT4, LeuP, ME (20 μM each), and catalyst **11** (4 μM) or riboflavin (4 μM) was photo-irradiated (λ = 500 nm) at 37 °C for 30 min, and each reaction mixture was analysed by LC-MS (n = 3, mean ± SEM, *: oxygenation yield at α-syn (1–6)).

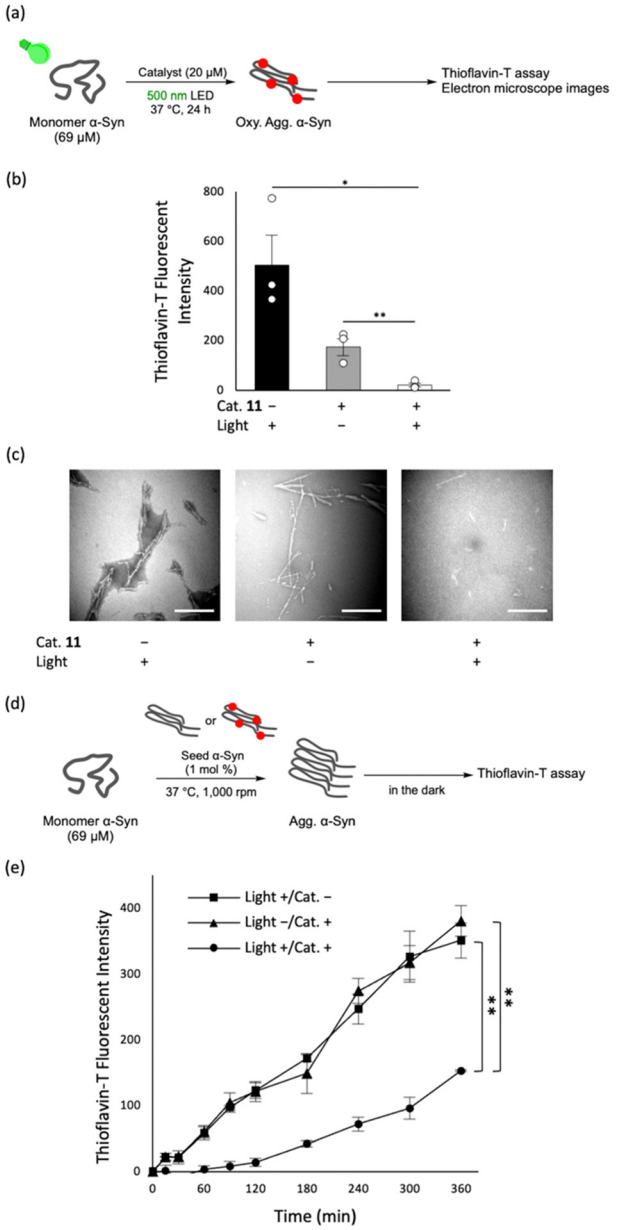

Fig. 3 (a) Experimental scheme to assess inhibitory effects of the catalytic photo-oxygenation on α-syn aggregation. A mixture of monomer α-syn (69 μM) was incubated with catalyst **11** (20 μM) or DMSO in PBS (pH 7.4) and irradiated with light at 500 nm at 37 °C for 24 h. After the reaction, aggregation degree of α-syn was evaluated. (b) ThT fluorescence assay in (a) (n = 3, mean ± SEM, *: $p < 0.05$, **: $p < 0.01$ by the Dunnett's test). The lower fluorescence intensity of ThT in the catalyst-only sample compared to the light-only sample is likely due to the competitive inhibition of ThT binding[18] to α-syn aggregates by catalyst **11**. (c) Electron microscope images in (a) (scale bar = 500 nm). (d) Experimental scheme of the seeding activity assay. Preformed seeds (1 mol% ratio) with or without photo-oxygenation using catalyst **11** were added to the monomer α-syn (69 μM). The following incubation was performed in the dark. (e) Aggregation degree with the incubation time in (d) was evaluated using ThT fluorescence assay. (n = 3, mean ± SEM, **: $p < 0.01$ by the Dunnett's test).

We then investigated effects of photo-oxygenation on the aggregation propensity of α-syn. α-Syn and catalyst **11** were incubated at 37 °C for 24 h under light irradiation (cat.+/light+), and the aggregation degree was evaluated using Thioflavin-T (ThT) whose fluorescence corresponds positively to the extent of cross-β sheet formation (Fig. 3a and b). Accordingly, the fluorescence intensity of ThT was significantly lower than that in the catalyst-only sample without photo-irradiation (cat.+/light−). The electron microscope analysis showed long and thick α-syn fibres in the catalyst-only sample (cat.+/light−), whereas α-syn fibrils were almost entirely absent in the

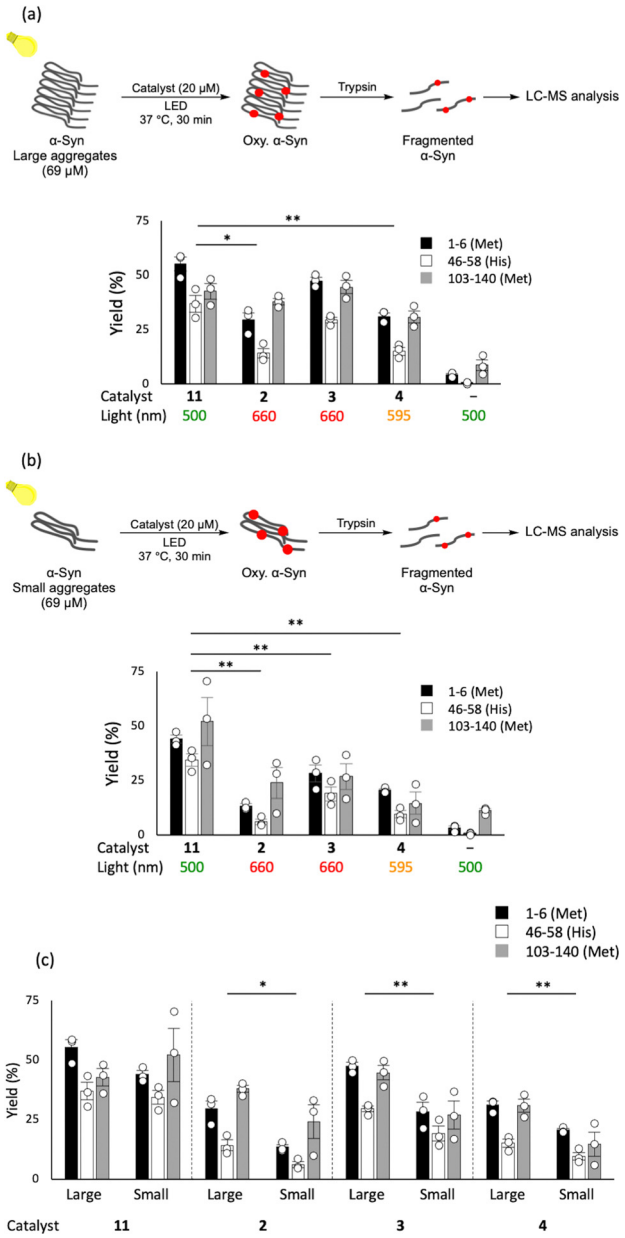

Fig. 4 (a) Photo-oxygenation yields of catalysts **2**, **3**, **4**, and **11** for α-syn large aggregates (n = 3, mean ± SEM, *: $p < 0.05$ in fragments 1–6 & 46–58, **: $p < 0.05$ in all fragments by the Dunnett's test). (b) Photo-oxygenation yields of catalysts **2**, **3**, **4**, and **11** for α-syn small aggregates (n = 3, mean ± SEM, **: $p < 0.05$ in all fragments by the Dunnett's test). (c) Comparison of photo-oxygenation yields of each catalyst for large *versus* small aggregates (n = 3, mean ± SEM, *: $p < 0.05$ in fragment 1–6 & 46–58, **: $p < 0.05$ in all fragments by the Dunnett's test).

photo-oxygenated sample (cat.+/light+; Fig. 3c). These results suggest that α-syn aggregation was inhibited by oxygenation.

Sonication of α-syn fibrils induces their fragmentation and the resulting smaller fibrils act as seeds to accelerate the aggregation of α-syn monomers.[19,20] We thus examined the effects of photo-oxygenation on seeding activity. Adding 1 mol% oxygenated or non-oxygenated α-syn seeds to a solution of α-syn monomer, we assessed time-dependent cross-β sheet propensities by ThT fluorescence intensity (Fig. 3d and e). The aggregation rate was significantly lower when oxygenated seeds were added (cat.+/light+) than when non-oxygenated seeds were added (cat.+/light−). This result indicates that the photo-oxygenation reduces the seeding activity of α-syn.

Finally, we compared the photo-oxygenation ability of catalyst **11** with the previous catalysts **2**, **3**, and **4** using two α-syn samples with distinct aggregation levels, designated as ''small aggregates'' (ThT fluorescence intensity was 106) and ''large aggregates'' (ThT fluorescence intensity was 1015) (Fig. 4). Those samples were prepared by shaking at 37 °C in 1000 rpm for 60 h and 120 h, respectively. Targeting large aggregates, **11** showed comparable activity to **3**, and higher activity than **2** and **4** (Fig. 4a). Targeting small aggregates, however, **11** was significantly more active than the other three catalysts (Fig. 4b). Only catalyst **11** oxygenated small and large aggregates equally well (Fig. 4c).

In conclusion, we identified photo-oxygenation catalyst **11** for α-syn amyloid, inspired by amyloid-sensing fluorescence probe **5**. Photo-oxygenation using **11** successfully inhibited α-syn aggregation. We revealed that the seeding activity of oxygenated α-syn was considerably lower than non-oxygenated α-syn. Furthermore, catalyst **11** oxygenated both small and large aggregates of α-syn with comparable activity. This feature is unique to **11**. Since small oligomers are highly neurotoxic, **11** might be a promising lead for the effective treatment of synucleinopathies.

We thank JSPS KAKENHI Grant Numbers JP20H00489 (M. K.), JP21H02602 (Y. S.), JP19H01015 and JP23H00394 (T. T.), JP18K06653, JP21H02622 and JP16H06277(CoBiA) (Y. H.), and AMED Grant Numbers JP21jm0210058h0004 (Y. S.), JP19dm0107106, JP19dm0307030 and JP22gm6410017 (Y. H.), JP19dk0207046, 22dm0207072 and 22dk0207061 (T. T.), and JST SPRING Grant Number JPMJSP2108 (A. I.).

A. I.: formal analysis, investigation, methodology, validation, writing – original draft. R. N.: investigation, methodology, validation. I. T.: investigation, methodology, validation. H. M.: investigation, validation, writing – review & editing. Y. H.: conceptualization, formal analysis, funding acquisition, investigation, supervision, validation writing – review & editing. T. T.: conceptualization, formal analysis, funding acquisition, investigation, supervision, validation writing – review & editing. Y. S.: conceptualization, formal analysis, funding acquisition, investigation, supervision, validation writing – review & editing. M. K.: conceptualization, formal analysis, funding acquisition, investigation, supervision, validation writing – review & editing.

Conflicts of interest

There are no conflicts to declare.

References

1 M. G. Spillantini, M. L. Schmidt, V. M. Lee, J. Q. Trojanowski, R. Jakes and M. Goedert, *Nature*, 1997, **388**, 839–840.
2 M. Baba, S. Nakajo, P.-H. Tu, T. Tomita, K. Nakaya, V. M.-Y. Lee, J. Q. Trojanowski and T. Iwatsubo, *Am. J. Pathol.*, 1998, **152**, 879–884.
3 C. M. Lema Tomé, T. Tyson, N. L. Rey, S. Grathwohl, M. Britschgi and P. Brundin, *Mol. Neurobiol.*, 2013, **47**, 561–574.
4 B. Li, P. Ge, K. A. Murray, P. Sheth, M. Zhang, G. Nair, M. R. Sawaya, W. S. Shin, D. R. Boyer, S. Ye, D. S. Eisenberg, Z. H. Zhou and L. Jiang, *Nat. Commun.*, 2018, **9**, 3609.
5 K. A. Conway, S.-J. Lee, J.-C. Rochet, T. T. Ding, R. E. Williamson and P. T. Lansbury, *Proc. Natl. Acad. Sci. U. S. A.*, 2000, **97**, 571–576.
6 B. Winner, R. Jappelli, S. K. Maji, P. A. Desplats, L. Boyer, S. Aigner, C. Hetzer, T. Loher, M. Vilar, S. Campioni, C. Tzitzilonis, A. Soragni, S. Jessberger, H. Mira, A. Consiglio, E. Pham, E. Masliah, F. H. Gage and R. Riek, *Proc. Natl. Acad. Sci. U. S. A.*, 2011, **108**, 4194–4199.
7 H. Braak, K. del Tredici, U. Rüb, R. A. I. de Vos, E. N. H. Jansen Steur and E. Braak, *Neurobiol. Aging*, 2003, **24**, 197–211.
8 M. Jucker and L. C. Walker, *Nature*, 2013, **501**, 45–51.
9 R. Cascella, S. W. Chen, A. Bigi, J. D. Camino, C. K. Xu, C. M. Dobson, F. Chiti, N. Cremades and C. Cecchi, *Nat. Commun.*, 2021, **12**, 1814.
10 A. Taniguchi, Y. Shimizu, K. Oisaki, Y. Sohma and M. Kanai, *Nat. Chem.*, 2016, **8**, 974–982.
11 J. Ni, A. Taniguchi, S. Ozawa, Y. Hori, Y. Kuninobu, T. Saito, T. C. Saido, T. Tomita, Y. Sohma and M. Kanai, *Chem*, 2018, **4**, 807–820.
12 T. Suzuki, Y. Hori, T. Sawazaki, Y. Shimizu, Y. Nemoto, A. Taniguchi, S. Ozawa, Y. Sohma, M. Kanai and T. Tomita, *Chem. Commun.*, 2019, **55**, 6165–6168.
13 N. Nagashima, S. Ozawa, M. Furuta, M. Oi, Y. Hori, T. Tomita, Y. Sohma and M. Kanai, *Sci. Adv.*, 2021, **7**, eabc9750.
14 S. Ozawa, Y. Hori, Y. Shimizu, A. Taniguchi, T. Suzuki, W. Wang, Y. W. Chiu, R. Koike, S. Yokoshima, T. Fukuyama, S. Takatori, Y. Sohma, M. Kanai and T. Tomita, *Brain*, 2021, **144**, 1884–1897.
15 Y. Liu, C. H. Wolstenholme, G. C. Carter, H. Liu, H. Hu, L. S. Grainger, K. Miao, M. Fares, C. A. Hoelzel, H. P. Yennawar, G. Ning, M. Du, L. Bai, X. Li and X. Zhang, *J. Am. Chem. Soc.*, 2018, **140**, 7381–7384.
16 C. H. Wolstenholme, H. Hu, S. Ye, B. E. Funk, D. Jain, C. H. Hsiung, G. Ning, Y. Liu, X. Li and X. Zhang, *J. Am. Chem. Soc.*, 2020, **142**, 17515–17523.
17 A. Taniguchi, D. Sasaki, A. Shiohara, T. Iwatsubo, T. Tomita, Y. Sohma and M. Kanai, *Angew. Chem., Int. Ed.*, 2014, **53**, 1382–1385.
18 S. A. Hudson, H. Ecroyd, T. W. Kee and J. A. Carver, *FEBS J.*, 2009, **276**, 5960–5972.
19 S. J. Wood, J. Wypych, S. Steavenson, J.-C. Louis, M. Citron and A. L. Biere, *J. Biol. Chem.*, 1999, **274**, 19509–19512.
20 M. Yonetani, T. Nonaka, M. Masuda, Y. Inukai, T. Oikawa, S. I. Hisanaga and M. Hasegawa, *J. Biol. Chem.*, 2009, **284**, 7940–7950.

